ELSEVIER

Journal of Molecular Catalysis A: Chemical 166 (2001) 73–85

JOURNAL OF MOLECULAR CATALYSIS A: CHEMICAL

www.elsevier.com/locate/molcata

Approximation of the Mulliken charges and dipole moments of the oxygen atoms of aluminophosphate sieves

A.V. Larin [a], D.P. Vercauteren [b,*]

[a] *Department of Chemistry, Moscow State University, Leninskie Gory, B-234, Moscow 119899, Russia*
[b] *Laboratoire de Physico-Chimie Informatique, Facultés Universitaires Notre Dame de la Paix, Institute for Studies in Interface Sciences, Rue de Bruxelles 61, B-5000, Namur, Belgium*

Received 22 September 1999; received in revised form 2 February 2000; accepted 16 February 2000

Abstract

Distributed multipole analysis on the basis of periodic Hartree–Fock (PHF)-type calculations, using the CRYSTAL95 code is applied to 12 aluminophosphate molecular sieves. Several approximations of the dependence of the Mulliken atomic charges and dipole moments of the crystallographically independent oxygen atoms calculated with the STO-3G, ps-21G*, and 6-21G* basis sets are obtained with respect to three oxygen parameters (i.e. average value and difference between the Al–O and P–O bond distances, and Al–O–P angle). Some deflections from these approximate forms for the different oxygen types are discussed.

Keywords: Mulliken charges; Dipole moments; Multipole analysis; Aluminophosphate

1. Introduction

Cationic forms of aluminophosphates are an important class of thermoresistant molecular sieves and are perspective candidates for numerous chemical applications. Recent studies with ab initio molecular dynamics confirmed the importance of the framework geometry for the activation of methanol [1]. Simultaneous analyses of the geometry for a wide series of molecular sieves should be performed together with the consideration of the resulting electrostatic field, as its influence on the decrease of the activation barrier of acetylene acylation has been recently presented [2]. Interestingly, these "geometry-field" relations provide the necessary data for less computing intensive methods like quantum mechanical/molecular mechanical methods [3], which require the knowledge of the electrostatic field and a correct estimation of the long-range interactions within molecular sieves such as zeolite frameworks. The electrostatic interactions clearly dominate in numerous adsorption processes within most of the aluminosilicates as it has been confirmed by both spectroscopic studies of adsorbed species [4] and theoretical estimations [5]. Close spatial structures between aluminophosphates and aluminosilicates a priori allow the importance of the electrostatic interactions within the aluminophosphate frameworks to be ascertained.

Usually the electrostatic field is only qualitatively simulated by the Mulliken charges [6,7]. However, the importance of the consideration of higher-order multipoles for a correct calculation of the interaction energy between CO adsorbed over a TiO_2 slab has been recently shown [8]. Point charges can be fitted if the field value is already known, for example, from periodic Hartree–Fock (PHF)-type calculations with the CRYS-

* Corresponding author. Fax: +32-81-72-45-30.

1381-1169/01/$ – see front matter
PII: S1381-1169(00)00455-6

TAL code [9]. Unfortunately, the latter approach can be hardly applied to estimate the field within frameworks with a large number of atoms per unit cell (UC) with arbitrary Si/Al or Al/P ratio also including compensatory ions, i.e. most of the zeolites which really present an interest within the most current industrial applications. Then alternative approaches to estimate the electrostatic field should be proposed.

In our previous studies [10,11], we used an approximate scheme, developed by Saunders et al. [6], of distributed multipole analysis related to the atomic positions within 14 all-siliceous analogues of aluminosilicate zeolites. The scheme [6] has been implemented in the CRYSTAL95 ab initio PHF LCAO code for periodic systems [9]. As it was shown [6], distributed multipole analysis allows to obtain electrostatic field values with a precision below 1% using multipole moments up to the fourth order. In our work, a common type of approximate dependence for the Mulliken charges (i.e. the moments of zeroth order within the scope of the scheme [6]) with different basis sets (STO-3G and 6-21G in [10], and ps-21G* in [11]) was proposed for each crystallographically independent type of oxygen and silicon atoms. More precisely, two-dimensional analytical functions with respect to the average Si–O distance and Si–O–Si angle [10] for O atoms and one-dimensional analytical functions with respect to the average Si–O distance [11] for Si atoms were derived. A comparison of the Si and O charges estimated with these analytical dependences confirmed their good agreement with results of large scale PHF-type calculations for all-siliceous mordenite [7] and silicalite [12]. Provided that such approximations in terms of the internal coordinates of each sieve atom could be obtained for higher multipole moments, electrostatic field values could be calculated precisely within any arbitrary all-siliceous zeolite.

Our approximate scheme is also a priori very appropriate for the case of aluminophosphates because the smaller P–O bond distances would lead to a sharper increase of the bielectronic integrals as compared to aluminosilicate frameworks [10,11]. Hence, the direct calculation with the PHF CRYSTAL95 code and a higher quality basis set even for an aluminophosphate framework with a moderate number of atoms per UC could be more expensive.

In this work, estimations of the dependences of the oxygen atomic charge and dipole moment are presented for 12 aluminophosphate (ALPO) structures with ratio $Al/P = 1$. This set of models was chosen because it does not require the consideration of any cation and it allows to apply the CRYSTAL95 code within a reasonable limit of computing time. The dependences for the O multipole moments together with analogous approximate dependences for the multipole moments of the Al and P atoms [13] could be the key to estimate the electrostatic field created by the atoms of larger frameworks whose direct solution is beyond the capabilities of the computing platforms and electronic structure codes currently available. Similar types of expressions for the multipole moments up to octupole for Al, P, and O atoms of the ALPO sieves are presently under study and will be presented in a future paper. The next step would then be to evaluate the field value for sieve contents of $Al/P > 1$ including cations.

In Section 2 of this paper, we discuss briefly the basis sets used together with the characteristics of the considered ALPO frameworks. In Section 3, we develop the approximate functions of the atomic O charges with respect to the internal parameters. In Section 4, approximations of such type of dependence of the O dipole moments are presented. The use of the two lowest multipole moments (i.e. charge and dipole) for the framework atoms leads to a better estimation of the electric field with respect to the one obtained by considering the Mulliken charges only as it will be demonstrated in the last section.

2. Theoretical aspects

The theoretical bases for the solution of the Hartree–Fock equation in three dimensions considering periodic boundary conditions have already widely been described in the literature [9,14,15]. The aluminophosphate structures were chosen on the basis of a relatively small number of atoms per elementary unit cell (UC). The characteristics of the 12 ALPO frameworks taken from the MSI database [16,17] are given in Table 1.

The minimal STO-3G basis set [20] was applied to all 12 considered systems. With the Durant–Barthelat pseudo-potential ps-21G* basis set for Al and P and 6-21G* for O [9] (named hereafter basis ps-21G*), and with the 6-21G* basis on all atoms, the SCF scheme converged properly for the AST, ATN, ATO, and CHA

Table 1
Symbol, number of atoms per unit cell (UC), of different Al, P ($n_P = n_{Al}$) and O types, of atomic orbitals (AO) per UC, and symmetry group of the aluminophosphate sieves [16,17], all of them corresponding to Al/P = 1

Name	Symbol[a]	Atoms/UC	n_{Al}/n_O	AO/UC (STO-3G)	Symmetry group
MAPO-39	ATN	24	1/4	152	I4
$AlPO_4$-16	AST	30	2/3	190	F23
$AlPO_4$-31	ATO	36	1/4	228	R3
$AlPO_4$-34[b]	CHA	36	1/4	228	R3
$AlPO_4$-11	AEL	60	3/11	380	Ibm2
$AlPO_4$-41	AFO	60	4/13	380	$Cmc2_1$
$AlPO_4$-18	AEI	72	3/12	456	C2/c
$AlPO_4$-5	AFI	72	1/4	456	P6cc
$AlPO_4$-12-TAMU	ATT	72	3/12	456	$P2_12_12$
$AlPO_4$-D	APD	96	4/16	608	$Pca2_1$
$AlPO_4$-C	APC	96	2/8	608	Pbca
$AlPO_4$-8	AET	108	5/19	684	$Cmc2_1$

[a] [18].
[b] [19].

sieves only. In the case of the ps-21G* basis, we optimised the exponents of the 3sp′ orbital of P and Al as 0.20 and 0.07 a.u.$^{-2}$, respectively, and of the 2sp′ orbital of O as 0.28 (instead of 0.13, 0.12 and 0.37 a.u.$^{-2}$, respectively, in [21]) for the AST structure. Too diffuse functions on Al led, however, to a slower SCF convergence, i.e. up to 20–25 iterations. We also optimised the exponents of the d polarisation functions as 0.5 and 0.25 a.u.$^{-2}$ for the P and Al atoms, respectively, and as 0.8 for oxygen. With the 6-21G* basis, the upper mentioned low 3sp′ exponent of Al appeared to be not appropriate. The sp′ and d exponents for Al, P, and O were again optimised as 0.14, 0.15, 0.45 and 0.35, 0.50, 0.72 a.u.$^{-2}$, respectively, in the case of AST.

All computations with the CRYSTAL95 code were realised on an IBM 15-node (120 MHz) scalable POWER parallel platform (with 1 Gb of memory/CPU). For all cases, the thresholds for the calculations were fixed to 10^{-5} for the overlap Coulomb, the penetration Coulomb, and overlap exchange, to 10^{-6} and 10^{-11} for the pseudo-overlap exchange, and to 10^{-5} for the pseudo-potential series for all levels of basis sets. The computations with the ps-21G* and 6-21G* basis were executed directly without keeping the bielectronic integrals files. The whole SCF convergence (9–10 cycles) requires around 50 and 70 min for AST (the same for ATN) within the ps-21G* and 6-21G* basis sets, respectively, and nearly three times more for the CHA and ATO sieves. The calculation of the respective moments takes usually below 6–7 min.

3. Approximation of the Mulliken atomic charges of the framework oxygens

Using the CRYSTAL95 code, 110 crystallographically independent atomic oxygen charge values were calculated with the minimal STO-3G basis set for all 12 studied aluminophosphate forms (ALPOs) (Table 1) and 15 different oxygen charge values for AST, ATN, ATO, and CHA sieves with the ps-21G* or 6-21G* bases. A representation of the O atomic charges as a function of the T_1–O–T_2 angle (ϑ) and average T–O distance $R = R(R_{OT_1} + R_{OT_2})/2$ (in Å) within several all-siliceous zeolite forms:

$$Q_0^0(R, \vartheta) = a_1 R^n + a_2 (R - R_0)^m \cos(\vartheta - \vartheta_0) \quad (1)$$

T_i corresponding to Si atoms, or herein to Al, P atoms, was already discussed [10,11]. The same representation is sufficient to reach a root mean square deviation (RMSD) of 2.73% between the STO-3G calculated values and the approximated ones within the ALPOs. The parameters of function (1) are given in Table 2. The differences between the calculated and the approximated Mulliken charges are presented in Fig. 1a.

Despite the particular important difference between the Al–O and P–O bond lengths is disregarded with function (1), the proposed approach leads to a rather good approximation as compared to a total charge variation of ±14% (Table 3). A better fit is achieved when all three coordinates characterising the internal

Table 2
Parameters of the approximate functions (Eqs. (1) and (2)) evaluated from the calculation, with STO-3G, ps-21G*, and 6-21G* basis sets, of N crystallographically independent oxygen charge values of the ALPO sieves

Equation	Basis set	N	a_1	n	$a_2 \times 10$	$R_0 \times 10^2$ (Å)	m	$\vartheta_0 \times 10^2$ (rad)	RMSD (%)
1	STO-3G	106	0.522	0.356	−0.152	113.1	−2.900	−1.408	2.73
2	STO-3G	110	2.414	−0.905	−0.678	−0.651	1.157	−0.150	1.55
2	ps-21G*	15	0.711	−0.032	−0.152	−0.652	0.453	−0.325	0.43
2	6-21G*	15	0.042	1.295	−0.012	−63.39	0.410	−2.693	1.45

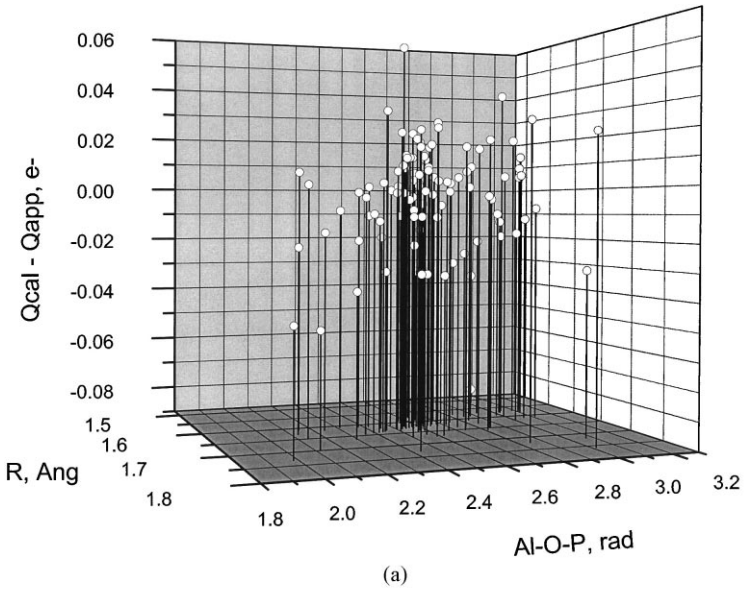

(a)

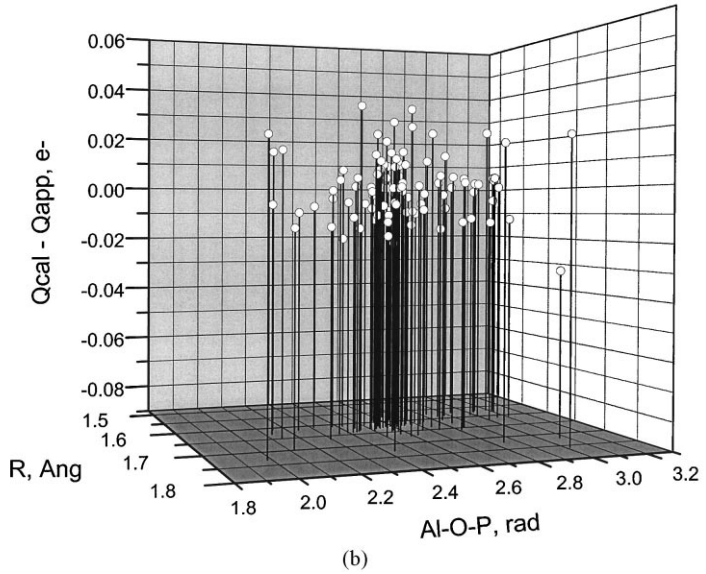

(b)

Fig. 1. Differences between the calculated Mulliken oxygen charges and the approximated ones (in $|e^-|$) obtained via (a) Eq. (1) and (b) Eq. (2) with respect to the internal coordinates, i.e. average distance R (in Å) and Al–O–P angle (in rad) of all ALPO frameworks.

Table 3
Variations of the oxygen atomic charge values of the ALPO sieves calculated with STO-3G, ps-21G*, and 6-21G* basis sets

Basis set	N	$Q^0_{\min}$	$Q^0_{\max}$	Range (%)	RMSD (%)
STO-3G	110	−0.8162	−0.6157	±14.0	1.55
ps-21G*	15	−0.9106	−0.8635	±2.8	0.43
6-21G*	15	−0.4107	−0.3661	±6.5	1.45

geometry of each O atom with respect to its neighbours are used. For convenience, we thus replaced the two different Al–O and P–O bond lengths by the average bond distance R upper mentioned and by the bond anisotropy $\Delta R = R_{\mathrm{OAl}} - R_{\mathrm{OP}}$ (in Å). A second modification of formula (1) was introduced allowing for a slightly better precision by considering an exponential function with respect to the average bond distance instead of a power presentation [11]. Finally, a six-parameter exponential form with a coupling term between the bond anisotropy ΔR and the angle Al–O–P was tested to fit the O charges in the considered ALPOs:

$$Q^0_0(R, \Delta R, \vartheta) = a_1\, \mathrm{e}^{nR} + a_2\, \mathrm{e}^{m(\Delta R - R_0)} \cos(\vartheta - \vartheta_0) \quad (2)$$

Eq. (2) allows to reach a better RMSD = 1.55% for the approximation of the Mulliken charges calculated with the STO-3G basis set (Table 2).

An interesting point is to analyse the variations of the three different contributions to the atomic charge obtained with the proposed function (2). The contribution of the "coupling" term between the angle Al–O–P and bond anisotropy ΔR, i.e. the last term in Eq. (2), is around 25% of the total charge value with the STO-3G and ps-21G* basis sets. The smaller values of the m parameter (Table 2) confirm a softer behaviour of function (2) with respect to the ΔR coordinate with a higher quality basis set. Hence, the exaggerated dependence on the internal coordinates obtained with the minimal STO-3G basis is useful to find a main functional form whose parameters would vary with the basis set applied.

The structure of the $AlPO_4$-34 sieve (CHA with Al/P = 1) optimised with a plane wave approach [19] was considered here together with other three-dimensional structures, obtained via X-ray diffraction. The respective charges and absolute values of the dipole moment (see Section 4) of the framework oxygens are satisfactorily fitted and do not demonstrate any particular behaviour. This justifies the choice of the ALPO structures studied herein, i.e. without any preliminary optimisation in order to find the geometry dependences. Earlier, it was shown that the O charges calculated with CRYSTAL for the optimised all-siliceous CHA zeolite [22] are in agreement with values coming from an analogous charge dependence approximation fitted using a set of non-optimised structures [10].

The differences between the charges calculated with CRYSTAL and the approximated ones using function (2) for the 110 crystallographically independent oxygen atoms within the studied ALPOs are presented in Fig. 1b. Evidently, the points fitted with (2) are located within a narrower slab close to zero as compared to those given in Fig. 1a. The distribution of the RMSD values with respect to the bond anisotropy ΔR does not reveal any correlation, which confirms the satisfactory choice of the dependence with respect to ΔR in Eq. (2). An average charge variation through all the ALPOs (Table 3) can be evaluated from the comparison between a simple one-dimensional linear fit (dotted line) and expression (2) (solid line) in Fig. 2 in the case of the STO-3G basis. The variations range to ±14 (Fig. 2a) and to ±2.8 and ±6.5% (Fig. 2b) for the STO-3G, ps-21G*, and 6-21G* bases, respectively, which is appreciable as compared to the respective RMSD values of 1.55, 0.43 and 1.45% obtained with function (2). A strong variation of the absolute charge values between the two split-valence basis sets is a consequence of a strong shift in the polarisation exponent for the Al atom. As the value 0.07 a.u.$^{-2}$ was not appropriate for the 6-21G* basis, a higher optimised value led to a serious change of the charges. In order to illustrate it, both split-valence basis sets with the same polarisation exponents were considered for the CHA case (as accepted for 6-21G*, see Section 2). The O charge values of −0.4504, −0.4361, −0.4562, −0.4376|e$^-$| obtained with ps-21G* are essentially closer to those calculated with the 6-21G*, i.e. −0.3883, −0.3740, −0.3941, −0.3759|e$^-$|, as compared to the charge values computed with a smaller Al exponent (ps-21G* case in Table 3). However, we considered the ps-21G* basis set for all four structures (AST, ATN, ATO, and CHA) with this small exponent value on Al,

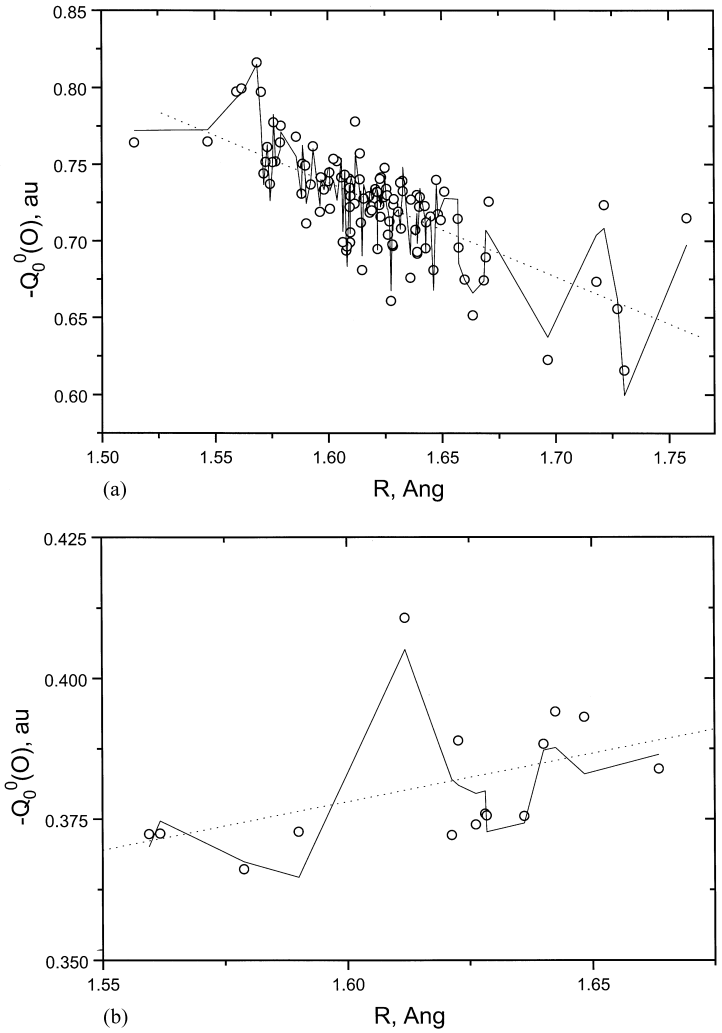

Fig. 2. Calculated Mulliken oxygen charges (in $|e^-|$) (circles) and approximated ones via linear one-dimensional function (dotted line) and Eq. (2) (solid line) with respect to the average distance R (in Å) for all ALPO frameworks: (a) STO-3G; (b) 6-21G*.

because the respective total energy for the CHA sieve was strongly more stable: −1847.3416 instead of −1846.6406 a.u. The lower absolute charge values are in agreement with the idea of more covalent bonds in the ALPO frameworks than in the all-siliceous systems [23].

One could suggest that the RMSD value of the charge approximation via function (2) is close to a lower precision limit considering that several characteristics of the respective Al and P neighbour atoms are not taken into account. Such characteristics are, for example, the average T–O distances which influence the atomic Mulliken charges [13] in the same manner as for the Si atoms [11], or the point symmetry group of the TO_4 tetrahedra. This limitation within approximation (2) could be indirectly proven via a closer analysis of the charges of the various O atoms presenting similar internal parameters and different deviation values from those obtained with function (2). This can be seen by analysing the AEI framework (Table 4), whose atomic charges are usually nicely approximated with Eq. (2). First, only three oxygen atoms among the

Table 4
Characteristics of several O, Al, and P atoms of the AEI and AST frameworks and deviations (charge error) between the Mulliken charges obtained with the STO-3G basis and the ones obtained using the approximate function (2) (respective parameters are given in Table 2)

Sieve	Oxygen type	R (Å)	ΔR (Å)	ϑ (°)	Neighbour atom types	AlO_4/PO_4 symmetries	Charge error (%)
AEI[a]	O(6)	1.6229	0.2110	147.4	Al(1)/P(3)	C_1/C_1	2.34
	O(10)	1.6229	0.2097	146.7	Al(2)/P(1)	C_{2v}/C_1	−0.97
	O(3)	1.6095	0.2110	150.5	Al(2)/P(2)	C_{2v}/C_1	−0.94
	O(4)	1.6390	0.2097	143.5	Al(2)/P(1)	C_{2v}/C_{2v}	1.67
AST[b]	O(2)	1.5595	0.2960	180.0	Al(1)/P(2)	C_{3v}/T_d	1.00
	O(3)	1.5618	0.3117	180.0	Al(2)/P(1)	T_d/C_{3v}	0.94
	O(1)	1.6119	0.3563	146.4	Al(1)/P(1)	C_{3v}/C_{3v}	2.50

[a] Numbering of the atoms is from [16,17].
[b] The same from [24].

12 different crystallographically independent types in AEI present charge deviations higher than the calculated RMSD = 1.55% (one of the oxygens is not presented in Table 4). Secondly, atoms O(6) and O(10) have very similar structural characteristics (Table 4). The estimation error using approximate form (2) is larger for O(6) linking two neighbour AlO_4 and PO_4 tetrahedra with a similar C_1 point symmetry group, as compared to O(10), for which the closest AlO_4 and PO_4 have different point symmetries. Thirdly, comparing O(3) and O(4) presenting different spatial characteristics, we observe a higher error for O(4) positioned between AlO_4 and PO_4 with a similar C_{2v} symmetry than for O(3) whose neighbour tetrahedra present C_{2v} and C_1 groups. Other examples of the relation between the symmetry and error value is given for the AST form (Table 4). A smaller error is indeed sought for the O(2) and O(3) charges connecting two TO_4 tetrahedra of different symmetries C_{3v} and T_d than for O(1) linking tetrahedra of the same symmetry (C_{3v}).

These observations of the influence of the TO_4 symmetry, completed below by one example in Section 4, require further studies, because they cannot be directly confirmed for all other frameworks, like AET and ATT, whose charges approximated by expression (2) are relatively poorer. No TO_4 tetrahedra within ATT present a C_1 symmetry, while all tetrahedra of AET are very close or correspond exactly to the C_{2v} symmetry. Considering the most precise O position in terms of symmetry coordinates relative to each type of tetrahedron surely would serve to find a more precise dependence.

4. Approximation of the dipole moments of the framework oxygens

The importance of the consideration of the field contribution from the atomic dipoles was shown in reference [8], wherein the electrostatic field above a TiO_2 surface was simulated with different approximation levels. We illustrate this by comparison of electrostatic potential (EP) values obtained with 6-21G* basis (Fig. 3a) relative to the EP representation at three levels based on the neglection of parts of the atomic multipole moments for the CHA framework. Generally, the inclusion of the moments up to fourth order should be sufficient for a correct calculation of the potential [6]. The three levels of the EP evaluation include Mulliken charges ($L = 0$ in Fig. 3b) on all atoms, charges and dipoles ($L = 0$ and 1 in Fig. 3c) on all atoms, and all atomic moments up to third order ($L = 3$ in Fig. 3d). The EP map was calculated in the Al–O(1)–P (angle 155.16°) plane of the CHA framework (Fig. 3a) applying the POTM option available in CRYSTAL95 [9]. In order to show the EP behaviour within an area available for a small adsorbed molecule, the EP was calculated within a space expanded by 4 Å (7.56 a.u.) from the Al–O side and from the right of the O–P side. The three highest peaks at the upper left corner in Fig. 3a correspond to the Al, O(1), and P atomic positions; the additional fourth peak of lower EP value comes from an oxygen located below the Al outside of the plane. As soon as the EP value of any atom displaced from the plane is lower than the one of the Al, O(1), and P atoms, the atom can be looked at a better resolution. In order to visualise the allowed

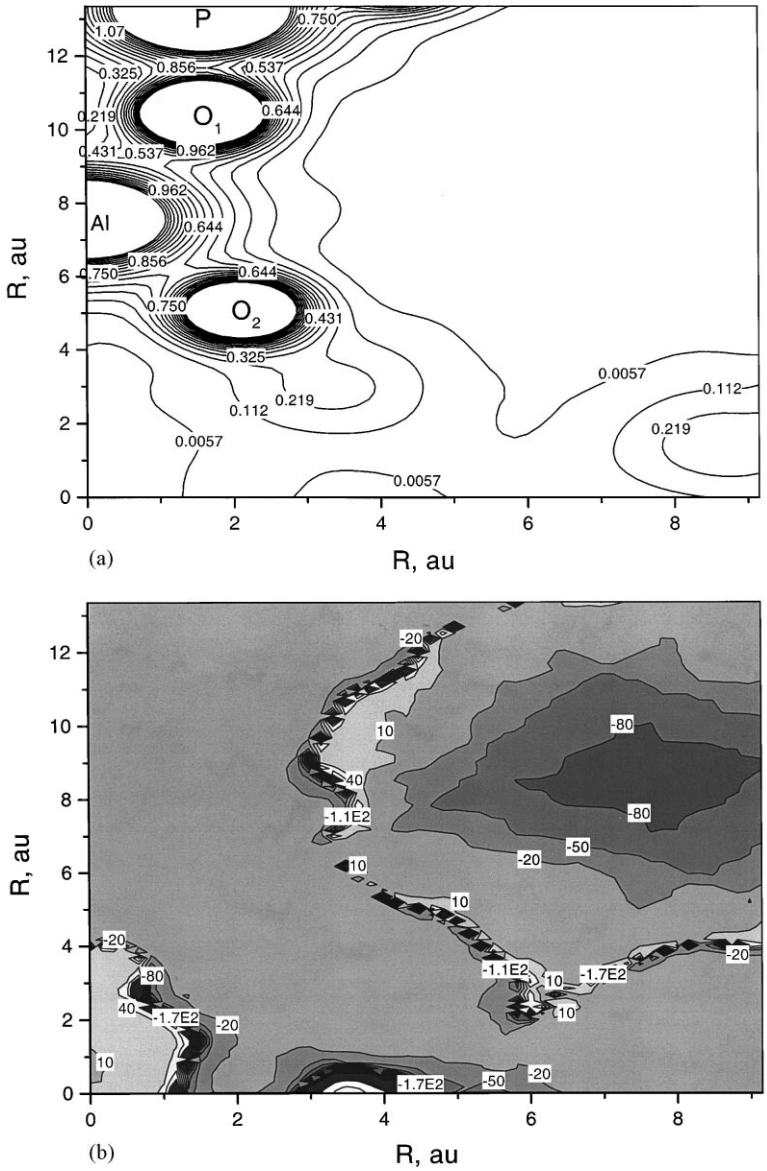

Fig. 3. (a) Electrostatic potential values EP(L) (a.u.) and EP differences presented as $(1 - \mathrm{EP}(L)/\mathrm{EP}(6)) \times 100$ (%) obtained with (b) Mulliken charges ($L = 0$) on all atoms, (c) charges and dipoles ($L = 0$ and 1) on all atoms, and (d) all atomic moments up to third order ($L = 3$) relative to the potential representation based on the sixth-order moments ($L = 6$). The moments are calculated with the 6-21G* basis sets with respect to the Al–O(1)–P plane of the CHA framework [19]. L value corresponds to the upper atomic moment considered for the EP calculation.

space within the plane, the all EP scale was limited by the range from 0 to 3 a.u. only. From this view, one immediately notices that a small adsorbed molecule can be located in the right upper corner corresponding to a plane passing between two adjacent four rings of the CHA.

Comparing Fig. 3b–d, one can see that the EP differences $(1-\mathrm{EP}(L)/\mathrm{EP}(6))$ are large along the area near

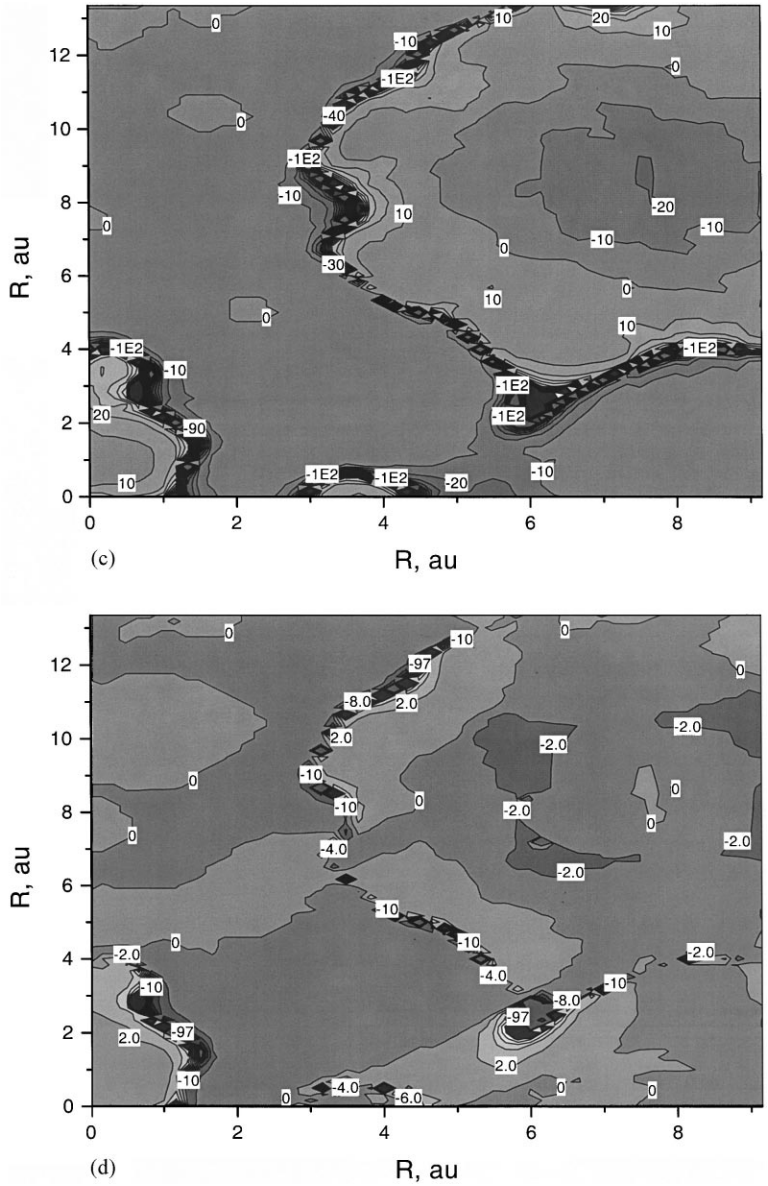

Fig. 3. (*Continued*).

the zero EP value (see Fig. 3a) with all three levels of computation (b–d). This cannot, however, be considered as a drawback of the three representations because even a negligible shift of the zero EP value should lead to a sharp EP difference. Then, on one hand, one can notice large differences between the $L = 0$ and $L = 0$ and 1 evaluations of the EP map in the above mentioned available part of internal space. If the charges only lead to EP differences up to 100% (b), the EP difference in case (c) does not exceed 20%. The EP map corresponding to the moments up to second order is not presented as it is only slightly better than the $L = 0$ and 1 EP map. On the other hand, a sharp improvement of the map quality is observed while

adding octupole moments as in the (d) case, which could be explained by the relative higher contributions of the third-order moments of the Al and P atoms. For their configurations which are close to tetrahedral ones, permanent non-zero electrostatic moment values lower than octupoles are forbidden. However, both T atoms have small dipoles and quadrupoles due to distortion of the AlO_4 and PO_4 tetrahedra. Speaking forward, the absolute dipole values are usually ordered as $Q_1(\mathrm{Al}) < Q_1(\mathrm{P}) < Q_1(\mathrm{O})$ [13] (see average dipole Q_1 notation below). The distortions lead to a more pronounced dipole on P in the smaller PO_4 unit than on the larger Al one. So, a better EP representation using only lowest moments ($L = 1$) is possible mainly due to the O contribution. This partly justifies that only O atoms were often intuitively used (together with cations if the zeolite or sieve has Al/Si and Al/P ratios different from unity) by researchers in computations within empirical and semi-empirical pair-wise addition schemes of the electric field influencing any adsorbed particle or molecule.

In order to derive a simple representation for the atomic dipole of zeolite oxygens, we first choose to determine its absolute value $Q_1 = ((Q_1^0)^2 + (Q_1^1)^2 + (Q_1^{-1})^2)^{1/2}$, where Q_L^m is the m-component of the L-order atomic multipole moment in a.u. [6,9]. We propose that the dipole of the O atom within a chemically bonded moiety Al–O–P should be proportional to the total dipole moment of this system represented crudely as an "isolated" one. The total dipole should be proportional to the bond anisotropy ΔR which leads to a non-zero dipole value even for the bond angle $\vartheta = \pi$. This means that terms proportional to ϑ and to ΔR should be considered separately in a first approximation. This simple idea allows us to propose a five-parameter expression with respect to two variables only ($\Delta R, \vartheta$) for all 106 atomic dipole values (not considering $AlPO_4$-34) calculated with the STO-3G basis:

$$Q_1(\Delta R, \vartheta) = a_1\, \mathrm{e}^{n(\Delta R - R_0)} + a_2 \sin(\vartheta - \vartheta_0) \qquad (3)$$

where $a_1 = 2.075$, $n = 1.0616$, $R_0 = 2.656$ Å, $a_2 = 0.048$, and $\vartheta_0 = -0.0282$ rad. Such approach provided a satisfactory RMSD value = 2.10%. A poorer coincidence was obtained with function (3) when considering rather long or too short average bond R values. The negative deviations for the longer average bond lengths and the positive deviations for the shorter ones were avoided by introducing an additional simple power term function of a third variable R:

$$Q_1(R, \Delta R, \vartheta) = a_1\, \mathrm{e}^{n(\Delta R - R_0)} + a_2 \sin(\vartheta - \vartheta_0) + a_3 (R - R_0')^m \qquad (4)$$

Fitting with Eq. (4) within the STO-3G basis resulted in RMSD = 1.67% and parameter values $a_1 = 1.272$, $n = 0.973$, $R_0 = 2.30$ Å, $a_2 = 0.0467$, $\vartheta_0 = -0.222$ rad, $a_3 = -0.3851$, $R_0' = 1.430$ Å, and $m = 3.038$. Any exponential function as a third term in Eq. (4) did not lead to a better result.

The absolute dipole values obtained within both split-valence bases could also be satisfactorily approximated using form (4). However, it seems to be excessive for such an approximation. The absolute values of the dipole moments calculated with the ps-21G* and 6-21G* basis sets decrease almost linearly with angle ϑ (Fig. 4 and Table 5). This proves an unsaturation of the STO-3G basis to represent O dipole values for higher bond angles. Despite a wide variation of the ΔR variable (Table 5), only terms proportional to the average distance R (but also small contribution) and angle ϑ in the right-hand side of Eq. (4) remains valid while fitting the dipole values. Respective parameters are shown in Table 6. The comparison between the m values confirms the softer geometry dependence with R of the O atomic dipole obtained with ps-21G* or 6-21G* versus those obtained with STO-3G. This is in line with the behaviour of the charge dependence via Eq. (2). However, considering the very wide variation of the dipole value (nearly ±70% around average value for both the series obtained with the two split-valence sets, Fig. 4), a simple function

$$Q_1(\vartheta) = a \sin\vartheta + b \qquad (5)$$

provides a precise enough estimation for the O dipole moments with RMSD of 8.4% ($a = 0.2112$, $b = 0.0263$) with ps-21G* and 6.2% ($a = 0.1385$, $b = 0.0255$) with 6-21G*. The reasons of such a difference between the computed moments and those approximated by means of formula (5) come from different points. For the dipole series computed with 6-21G*, the deviations of −16 and 13% comes from O(3) of AST and O(2) of ATO with moderate angles of 146.4 and 162.9°, respectively. In ps-21G*, two serious deflections of 11 and 25% correspond to small dipole

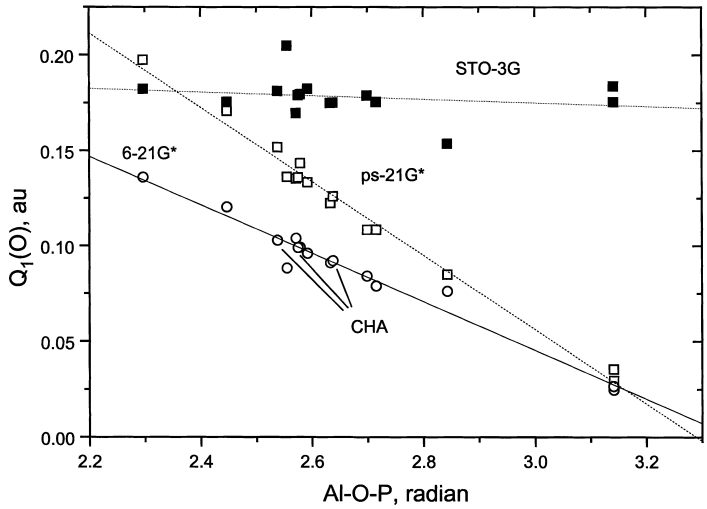

Fig. 4. Absolute dipole moments calculated with the STO-3G (filled squares), ps-21G* (open squares), and 6-21G* (circles) basis sets with respect to Al–O–P angle. Linear approximations are given by dotted, dashed, and solid lines, respectively. Oxygen dipole values for the optimised CHA structure are marked for the 6-21G* basis.

for ϑ near 180° for O(2) and O(3) of AST, as already discussed for the atomic charge in Section 3 (Table 4). The latter present analogous internal geometries but opposite AlO_4 and PO_4 tetrahedral symmetries (C_{3v} or T_d). We hope that a final explanation of the deviations of the approximated O(2) and O(3) dipoles versus the calculated ones could be proposed together with a closer analysis of the Al and P dipole moments, which is presently under study [13]. A priori, the high differences with the fitted dipole values could be qualitatively explained through a strict T_d symmetry of the neighbour TO_4 tetrahedra. In order to demon-

Table 5
Absolute dipole moment values Q_1 of four ALPO sieves calculated with STO-3G, ps-21G* and 6-21G* basis sets with respect to the average bond length R, bond anisotropy ΔR, and Al–O–P angle

Type	R (Å)	ΔR (Å)	ϑ (rad)	ps-21G*	6-21G*	STO-3G
AST	1.5595	0.2960	3.1416	0.02958	0.02473	0.17553
	1.5618	0.3117	3.1413	0.03552	0.02662	0.18377
	1.6119	0.3563	2.5548	0.13630	0.08835	0.20487
ATN	1.5788	0.2424	2.6987	0.10843	0.08408	0.17883
	1.5900	0.1988	2.6332	0.12247	0.09109	0.17494
	1.6213	0.2238	2.7150	0.10843	0.07886	0.17545
	1.6227	0.2196	2.5920	0.13335	0.09596	0.18231
ATO	1.6284	0.1348	2.5712	0.13531	0.10394	0.16963
	1.6361	0.1271	2.4468	0.17077	0.12034	0.17553
	1.6484	0.1392	2.8431	0.08493	0.07613	0.15369
	1.6636	0.1459	2.2967	0.19746	0.13601	0.18231
$AlPO_4$-34	1.6262	0.2000	2.5789	0.14341	0.09916	0.17950
	1.6281	0.2007	2.5377	0.15183	0.10286	0.18119
	1.6401	0.2086	2.6377	0.12599	0.09212	0.17512
	1.6425	0.2083	2.5751	0.13591	0.09902	0.17904

Table 6
Parameters of approximate function (Eq. (4) without the first term proportional to ΔR) evaluated using 15 crystallographically independent oxygen dipoles of ALPO sieves with the ps-21G* and 6-21G* basis sets

Basis set	a_2	ϑ_0 (rad)	a_3	R'_0 (Å)	m	RMSD (%)
ps-21G*	−0.2235	2.224	0.2313	1.559	0.0374	3.9
6-21G*	−0.1311	2.159	0.1644	1.488	0.0293	5.8

strate this, let us again consider an "isolated" fragment Al–O–P whose total dipole moment is related to the oxygen. An expression for any central moment Q_L (which we can assign to the oxygen) of this moiety through local moments Q_l of lower or equal order $l \leq L$ was developed by Stone (formula (11) in [25]). Zeroth values of all multipole moments Q_L, $L < 3$, on the T atom within TO_4 tetrahedra of T_d symmetry [26] lead to a smaller total multipole of the same order on the central O atom. Within AST, the contributions to the central dipole moment will be zero from the local P(2) dipole moment for the O(2) dipole, or from the local Al(2) dipole moment for O(3). The difference between the atomic dipole values of Al and P is the reason of the contrary signs of the dipole deflections obtained with approximate function (4). That is why this simple analysis requires a more detailed explanation including Al and P representations.

Another useful point to remark is related to the comparison of the optimised (CHA from [19]) and non-optimised (AST, ATN, ATO) models for a common search of the dependences. Only the CHA model has been optimised, that is why all models are used together with results of X-ray experiments considered without further optimisation. The behaviour versus the Al–O–P angle of the respective four O dipole values of CHA, ranging between 145.53 and 151.16 (2.54 and 2.64 rad in Fig. 4), is similar to the one of the other structures (we did not mark them by separate symbols for simplification in Fig. 4). Evidently, the parameters of the approximate dependences should be more reliable than those obtained after fitting of the moments related to "raw" (non-optimised) zeolite models, but it should not lead to any serious quantitative difference.

Ideally, the approximation for the estimation of the O dipole moment shown herein should be complemented by an analogous representation of the upper atomic moments in order to obtain a more precise presentation as in Fig. 3d. Similar type of analytical expressions for all components of the dipole and upper moments up to octupole for O, Al, and P atoms are possible. This work is actually under progress.

5. Conclusion

A distributed multipole analysis on the basis of periodic Hartree–Fock calculations with three levels of basis sets, the minimal STO-3G, a split-valence including pseudo-potential (Durant–Barthelat) ps-21G* basis on aluminium and phosphorus and 6-21G* on oxygen, and the split-valence 6-21G* on all atoms, via the CRYSTAL95 code was considered for 12 aluminophosphate (ALPO) molecular sieves with ratio Al/P = 1. With the extended basis set, convergence of the SCF procedure could be reached for the sieves AST, ATN, ATO, and $AlPO_4$-34 only. 110 and 15 Mulliken atomic O charges for the crystallographically independent O types were computed with the STO-3G and ps-21G*or 6-21G* basis sets, respectively. Their analysis were then performed in terms of three internal parameters, the average T–O distance (T = Al, P), the T–O bond anisotropy, and the Al–O–P bond angle of the framework oxygens. The best fitting of the O charges is obtained via a six-parameter approximate expression (Eq. (2)).

An analogous five-parameter approximate function (Eq. (4) without first term in the right-hand side) for the absolute dipole moment value of the O atoms was obtained first with respect to the same three internal coordinates as for the Mulliken O charges. A higher importance of the term corresponding to the angular dependence of the dipole was, however, observed with the split-valence bases as compared to the STO-3G one. Several deviations of the approximate function values for both the O charges and dipole moments here calculated were observed for different symmetries of the two closest neighbour TO_4 tetrahedra. Further studies of the relation between the TO_4 symmetry variation and charge values would be useful to derive more precise expressions.

The fitting with function (4) may be considered as a first satisfactory approximation of the multipole moments of orders higher than zero (i.e. of the charges) for all O framework atoms. It suggests that approximate functions could also be fitted for other higher

moments assuming a deeper theoretical approach to search the respective functions. Then a precise representation of the electrostatic field within frameworks with a larger number of atoms per unit cell would be possible even if one cannot calculate the respective field directly with codes such as CRYSTAL.

Both the approximate forms for the charges and dipole moment could be useful for the field estimations in any ALPO framework while constructing embedded model or using empirical simulation of any ALPO sieve.

Acknowledgements

The authors wish to thank the FUNDP for the use of the Namur Scientific Computing Facility (SCF) Centre, a common project between the FNRS, IBM-Belgium, and FUNDP. They acknowledge financial support of the FNRS-FRFC, the "Loterie Nationale" for the convention no. 9.4595.96, and MSI for the use of their data in the framework of the "Catalysis and Sorption" consortium. AVL acknowledges the PAI 4-10, the "Services du Premier Ministre des Affaires Scientifiques, Techniques et Culturelles" of Belgium for his Postdoctoral stage and the Russian Foundation of Basic Researches for financial support (Grant no. 96-03-33771).

References

[1] I. Stich, J.D. Gale, K. Terakura, M.C. Payne, Chem. Phys. Lett. 283 (1998) 402.
[2] P. Dziekónski, W.A. Sokalski, E. Kassab, M. Allavena, Chem. Phys. Lett. 288 (1998) 538.
[3] M. Brändle, J. Sauer, J. Mol. Catal. A 119 (1997) 19.
[4] E. Cohen de Lara, Y. Delaval, J. Chem. Soc., Faraday Trans. 64 (1978) 790.
[5] A.M. Ferrari, P. Ugliengo, E. Garrone, J. Chem. Phys. 105 (1996) 4129.
[6] V.R. Saunders, C. Freyria-Fava, R. Dovesi, L. Salasco, C. Roetti, Mol. Phys. 77 (1992) 629.
[7] J.C. White, A.C. Hess, J. Phys. Chem. 97 (1993) 6398.
[8] P. Reinhardt, M. Causà, C.M. Marian, B.A. Heß, Phys. Rev. B 54 (1996) 14812.
[9] R. Dovesi, V.R. Saunders, C. Roetti, M. Causà, N.M. Harrison, R. Orlando, E. Aprà, CRYSTAL95 1.0, User's Manual, University of Torino, 1996.
[10] A.V. Larin, L. Leherte, D.P. Vercauteren, Chem. Phys. Lett. 287 (1998) 195.
[11] A.V. Larin, D.P. Vercauteren, Int. J. Quant. Chem. 70 (1998) 993.
[12] J.C. White, A.C. Hess, J. Phys. Chem. 97 (1993) 8703.
[13] A.V. Larin, D.P. Vercauteren, Submitted to Chem. Phys. Lett.
[14] C. Pisani, R. Dovesi, C. Roetti, Hartree–Fock Ab Initio Treatment of Crystalline Systems, Springer, New York, 1988.
[15] A.C. Hess, V.R. Saunders, J. Phys. Chem. 96 (1992) 4367.
[16] J.M. Newsam, M.M.J. Treacy, ZeoFile — a stack of zeolite structure types, Catalysis and Sorption Software and Databases, Molecular Simulations Inc., San Diego, CA, 1995.
[17] J.M. Newsam, M.M.J. Treacy, Zeolites 13 (1993) 183.
[18] R.M. Barrer, Pure Appl. Chem. 51 (1979) 1091.
[19] Y. Jeanvoine, J.G. Ángyán, G. Kresse, J. Hafner, J. Phys. Chem. B102 (1998) 5573.
[20] W.J. Hehre, L. Radom, P.V.R. Schleyer, J.A. Pople, Ab Initio Molecular Orbital Theory, Wiley, New York, 1986.
[21] M. Causà, Supplied materials for the CRYSTAL95, available through http://www.dl.ac.uk/TCS/Software/CRYSTAL.
[22] E. Aprà, R. Dovesi, C. Freyria-Fava, C. Pisani, C. Roetti, V.R. Saunders, Model. Simul. Mater. Sci. Eng. 1 (1993) 297.
[23] L. Uytterhoeven, W.J. Mortier, P. Geerlings, J. Phys. Chem. Solids 50 (1989) 479.
[24] J.M. Bennett, B.K. Marcus, Stud. Surf. Sci. Catal. 37 (1987) 269.
[25] A.J. Stone, Chem. Phys. Lett. 81 (1981) 233.
[26] S. Bhagavantam, D. Suryanarayana, Acta Cryst. 2 (1949) 21.